PCCP

Accepted Manuscript

ROYAL SOCIETY OF CHEMISTRY

www.rsc.org/pccp

Enhancement of thermoelectric figure of merit in DNA-like systems induced by Fano and Dicke effects

Hua-Hua Fu,* Lei Gu, Dan-Dan Wu and Zu-Quan Zhang

College of Physics and Wuhan National High Magnetic field center, Huazhong University of Science and Technology, Wuhan 430074, People's Republic of China

*E-mail: hhfu@hust.edu.cn

Abstract

We report a theoretical study highlighting the thermoelectric properties of biological and synthetic DNA molecules. Based on an effective tight-binding model of duplex DNA and by using the nonequilibrium Green's function technique, thermal conductance, electrical conductance, Seebeck coefficient and thermoelectric figure of merit in the system are numerically calculated by varying the asymmetries of the energies and the electronic hoppings in the backbone sites to simulate the environmental complications and fluctuations. We find that due to the multiple transport paths in the DNA molecule, the Fano antiresonance occurs, and enhances the Seebeck coefficient and the figure of merit. When energy difference in every opposite backbone site is produced, the Dicke effect appears. This effect gives rise to a semiconducting-metallic transition, and enhances the thermoelectric efficiency of the DNA molecule remarkably. Moreover, as the Fano antiresonance point is close to the Dicke resonance one, a giant enhancement in thermoelectric figure of merit in the DNA molecule has been found. These results provide a scenario to obtain effective routes to enhance the thermoelectric efficiency in the DNA molecules, and suggest perspectives for future experiments intending to control the thermoelectric transport in DNA-like nanodevices.

Keywords: thermoelectric figure of merit, Fano effect, Dicke effect, DNA-like systems

(Some figures may appear in colour only in the online journal)

I. Introduction

Very recently, the deoxyribonucleic acid (DNA) molecule has attracted considerable attention from the physics, chemistry, and biology communities,[1] due to its superior self-assembly properties in living organism and a promising candidate for molecular electronics.[2] Since the original proposal by Eley and Spivey that the DNA molecule could provide a natural pathway for conducting electrons,[3] a number of experimental groups reported the measurements of charge migration along duplex DNA molecule, and demonstrated that the DNA has proximity-induced superconducting,[4] metallic,[5-7] semiconductor,[8-10] and insulating behaviors,[11-13] mainly on poly(G: guanine)-poly(C: cytosine) and λ-NDA molecules. These rich transport behaviors stem from a wide range of experimental complications, including the DNA samples, counterions, humidity, interaction of DNA with substrate, and different situations of contacts between DNA and electrodes. To understand the experimental observations, it has already realized that three different contributions on the DNA molecule, i.e., the neucleobaes (basespairs) in DNA, the presence of backbones and the influence of environment, should be taken into account.[14-17] On the other side, to grasp the underlying transport mechanisms, various theoretical approaches have been adopted.[18-27] For example, *ab initio* calculations predict that synthetic poly(G)-poly(C) is a semiconductor.[28] While the tight-binding Hamiltonian model in the DNA molecule shows that the rich transport behaviors are relative to different mechanisms, such as hybridization between base pairs and sugar-phosphate,[14] interbase Coulomb repulsion,[29] backbone-induced electronic effects,[17] and dimensionality-induced effects.[28] Besides, a very recent experimental observation shows that a high spin selectivity of photoelectron transmission appears in self-assembled monolayers of double-stranded DNA molecule.[30] To understand the high spin polarizations, the spin-orbit coupling, the environment-induced dephasing and the helical symmetry should be considered together.[27,31] Whereafter a generation of pure spin currents by electric field driving is also proposed in the DNA molecule.[32] These works provide the possibility of a deeper understanding of spin-selective processes in biology.[33]

It is obvious that in the previous works, the electron or spin-dependent transport properties in the DNA molecule have been mainly investigated, while the findings enrich organic electronics and spintronics largely. To broaden the device applications on the DNA molecule, it is natural to ask whether the DNA molecule can be applied as good thermoelectric devices, and what mechanisms can enhance the thermoelectric efficiency in it. Motivated by these, in the present work, we devote to study the thermoelectric properties in the DNA molecule, though they have less been reported so far. Considering the particular double-stranded structures in the DNA molecule composed of lots of nucleobases and backbone sites, much more Feynman paths for the electron transmission are provided, thus quantum interferences of electron waves occur easily in passing through the DNA systems.[34-36] As a result, the Mott relation and the Wiedemann-Franz (WF) law, which are two factors to suppress the thermoelectric figure of merit, may be violated.[37] Thus, an effective route to enhance the figure of merit of the DNA systems is achieved. Our theoretical results show that due to the dangling backbones in every nucleobase, the Fano antiresonance occurs,[38] leading to the fact that the thermal electronic conductance is much suppressed. Meanwhile, if considering the energy difference between the upper and lower backbones induced by environmental complications or fluctuations, the Dicke resonance effect occurs,[39,40] giving rise to a semiconducting-metallic transition. More important, the both interference effects enhance the thermoelectric figure of merit of the DNA molecule remarkably. Our study provides a scenario to obtain effective routes to enhance the thermoelectric efficiency in the DNA molecule, and suggest perspectives for future experiments intending to control the thermoelectric transport through DNA-like nanodevices.

The reminder of this work is organized as follows. In Section 2, we construct a theoretical model to describe the poly(G)-poly(C) DNA molecule and present some analytical expressions for the thermoelectric properties by using the non-equilibrium Green's function technique. Then we discuss the Fano and Dicke effects in the DNA molecule, and explore their influences on the figure of merit and the Seebeck coefficient in Section 3. Finally, we make a brief conclusion in Section 4.

II. Model and theoretical method

According to quantum chemistry studies on duplex DNA that the hydrogen bonding between complementary nucleobases is larger than the π stacking energies between successive base pairs, each Watson-Crick base pair can be treated approximatively as a single entity with a characteristic on-site energy.[41,42] A detailed understanding of the DNA structure suggests that π-π interaction between the stacked base pairs in the DNA molecule could support extended charge transport. Moreover, the electronic couplings though a duplex stack of nucleobases are expected to involve both intrastrand and interstrand pathways.[43] Therefore a physically reasonable description of charge transport in duplex DNA including the backbone structure would be Fishbone model.[14,44] Here we choose poly(G)-poly(C) oligomer as a typical sequence which has been investigated widely in experiment and theory.[45-47] As illustrated in Figures 1(a) and 1(b), the poly(G)-poly(C) DNA molecule in the Fishbone model has one central conduction channel in which individual sites represent a G:C base-pair, which are interconnected and further linked to upper and lower backbones, but are not interconnected along the backbones.[14] In the presence of the left and right thermal contacts, the Hamiltonian can be described as

$$H = H_{\mathrm{L}} + H_{\mathrm{R}} + H_{\mathrm{DNA}} + H_{\mathrm{Coup}}, \tag{1}$$

where $H_{\mathrm{L(R)}}$ represents the Hamiltonian of the left (right) thermal contact and can be expressed as $H_{\alpha(=\mathrm{L,R})} = \sum_{\alpha k\sigma} \varepsilon_{\alpha k\sigma} c^{\dagger}_{\alpha k\sigma} c_{\alpha k\sigma}$, where $c^{\dagger}_{\alpha k\sigma}$ ($c_{\alpha k\sigma}$) is the creation (annihilation) operator of the electrons with momentum k, spin index σ ($\sigma = \uparrow, \downarrow$ or $\sigma = \pm 1$) and energy $\varepsilon_{\alpha k\sigma}$ in the lead-α (α = L, R). The Hamiltonian of the poly(G)-poly(C) DNA molecule, i.e., H_{DNA}, may be described as follows,[14]

$$H_{\mathrm{DNA}} = \sum_{i,\sigma} \varepsilon_h d^{\dagger}_{i,\sigma} d_{i,\sigma} + \sum_{\langle i,j\rangle,\sigma} t_0 d^{\dagger}_{i,\sigma} d_{j,\sigma} + \sum_{i,\sigma,\beta} \varepsilon_{i,\beta} a^{\dagger}_{i,\sigma,\beta} a_{i,\sigma,\beta} + \sum_{i,\sigma,\beta=\pm} t_{i,\beta} (a^{\dagger}_{i,\sigma,\beta} d_{i,\sigma} + \mathrm{H.c.}). \tag{2}$$

Here, $d^{\dagger}_{i,\sigma}$ ($d_{i,\sigma}$) and $a^{\dagger}_{i,\sigma,\beta}$ ($a_{i,\sigma,\beta}$) denotes the creation (annihilation) operators of an electron with spin σ at site i in the GC base pair and in the backbone, with index $i \in [1, N]$ labeling a nucleotide

and index $\beta = \pm$ labeling an upper or lower backbone sites. ε_h and $\varepsilon_{i,\beta}$ are the on-site energies of the GC base pair and the backbone, respectively. t_0 is the hoping integral along the GC base pairs and $t_{h,\beta}$ gives the hopping integral from each site on the GC base pairs to the upper or lower backbone. The last one in Eq. (1) denotes the coupling between the DNA molecule and the contacts, and takes the form

$$H_{\text{Coup}} = \sum_{k,\sigma} (V_{Lk\sigma} c^{\dagger}_{Lk\sigma} d_{1,\sigma} + V_{Rk\sigma} c^{\dagger}_{Rk\sigma} d_{N,\sigma} + \text{H.c.}), \tag{3}$$

where $V_{\alpha k\sigma}$ denotes the coupling strength between the contacts and the left ($\alpha = L$) and right ($\alpha = R$) base pair. In the calculations, the coupling between the contact and the base pair is described usually by the width function $\Gamma_\alpha = 2\pi |V_{\alpha \text{k}}|^2 \rho_\alpha(\omega)$, where $\rho_\alpha(\omega)$ is the density of states in the contact-α. Here, we will ignore the ω dependence of Γ_L since the density of states (DOS) in the left contact, $\rho(\omega)$, can be usually viewed as a constant. Similarly, we can define Γ_R, the coupling coefficient associated with the right contact. Because we only consider the symmetric coupling between the contacts and the DNA molecule by the assumption $V_{Lk} = V_{Rk} = V$.

Assume that the bias voltage difference ΔV as well as the temperature gradient ΔT are applied in two contacts. The linear response theory gives the following formulas for the charge, spin and heat currents:

$$I^c = \sum_\sigma I_\sigma = e^2 \sum_\sigma L_{0\sigma} \Delta V + \frac{e}{T} \sum_\sigma L_{1\sigma} \Delta T, \tag{4}$$

$$I^s = \sum_\sigma I^s_\sigma = \frac{\hbar}{2} \sum_\sigma \sigma L_{0\sigma} \Delta V + \frac{\hbar}{2T} \sum_\sigma \sigma L_{1\sigma} \Delta T, \tag{5}$$

$$I^Q = \sum_\sigma I^Q_\sigma = \sum_\sigma L_{1\sigma} \Delta V + \frac{1}{T} \sum_\sigma L_{2\sigma} \Delta T. \tag{6}$$

It should be noted that in the linear response regime, both ΔV and ΔT approach to zero. The above three thermoelectric coefficients are expressed in terms of quantities $L_{n\sigma}$, which can be easily determined by the following relation

$$L_{n\sigma} = -\frac{1}{\hbar}\int \frac{d\omega}{2\pi}(\omega - E_f)^n T_\sigma(\omega)\frac{\partial f_\alpha(\omega)}{\partial \omega}, \quad (7)$$

where $f_\alpha(\omega)$ corresponds to equilibrium Fermi-Dirac function having the form of $f_\alpha(\omega) = \{\exp[(\omega - \mu_\alpha)/k_B T_\alpha] + 1\}^{-1}$, where μ_α and T_α denote the corresponding chemical potential and temperature, and k_B indicates the Boltzmann constant. Moreover, E_F is the Fermi energy and $T_\sigma(\omega)$ describes transmission probability through the GC base pairs along the DNA molecule, which can be expressed by the Fourier transform of Green's functions of the DNA molecule and by the coupled matrices Γ_α (α = L, R) through the expression $T_\sigma(\omega) = \mathrm{Tr}[\mathrm{G}^a_\sigma(\omega)\Gamma_R(\omega)\mathrm{G}^r_\sigma(\omega)\Gamma_L(\omega)]$, where $\mathrm{G}^{r(a)}_\sigma(\omega)$ is retarded (advance) Green's function,[48,49] which can be calculated by the equation of motion technique.[50,51]

The Seebeck coefficient S is defined as the ratio of the voltage drop ΔV generated by the temperature difference ΔT, $S = \Delta V/\Delta T$, taken in the absence of charge current, $I^c = 0$. Thus, considering the above equations, the liner electronic conductance G, the Seebeck coefficient S, and the electronic thermal conductance κ_e can be defined as the following[52,53]

$$G = e^2 \sum_\sigma L_{0\sigma}, \quad (6)$$

$$S = \left(\frac{\Delta V}{\Delta T}\right)_{I^c=0} = -\frac{1}{eT}\frac{\sum_\sigma L_{1\sigma}}{\sum_\sigma L_{0\sigma}}, \quad (7)$$

$$\kappa_e = \frac{1}{T}\left[\sum_\sigma L_{2\sigma} - \frac{(\sum_\sigma L_{1\sigma})^2}{\sum_\sigma L_{0\sigma}}\right]. \quad (8)$$

It should be noted that the thermal conductance is determined on the condition of vanishing charge current. Thus, to determine the basic thermoelectric properties, we need to calculate out all the relevant integrals $L_{n\sigma}$ (n = 0, 1, 2). Then we can get the figure of merit (ZT) of the DNA system as $ZT = (S^2 GT)/\kappa$, where κ is the thermal conductance, which is contributed by the electric thermal conductance κ_e and the lattice (phonon) thermal conductance κ_{ph}, i.e., $\kappa = \kappa_e + \kappa_{ph}$.

Considering that the temperature set in the device is low remarkably and that the linear-response regime is adopted, the thermal conductance contributed by lattice vibrations is little and thus neglected in the calculations firstly. These formulas presented above will be used to calculate the related thermoelectric coefficients.

III. Results and discussion

In this section, we will present the results of our numerical computations. In the calculations, we set $\rho(\omega) = 1$, and set the chemical potentials of the left and right contacts to be $\mu_L = eV/2$ and $\mu_R = -eV/2$, respectively, where $e\Delta V = \mu_L - \mu_R$ denotes the applied bias voltage. It is assumed that the DNA molecule is symmetrically coupled to the contacts with $\Gamma_L = \Gamma_R = t_0$, indicating a relatively strong coupling. Before we proceed, we need to introduce the coupling parameter t_0 as the energy unit, and consider a very low device temperature $k_BT = 0.01t_0$, because relatively high device temperature suppresses the quantum interference effects and reduces the figure of merit of the system.[54] In addition, we assume that the system has a uniform Fermi energy E_f which is set as zero, and for convenience, we set $e = \hbar = 1$ in the calculations.

First of all, let us focus on the influence of the Fano antiresonance on the thermoelectric properties of the DNA molecule. For simplicity, we consider here a homogeneous DNA chain with $\varepsilon_h = \varepsilon_0$, $\varepsilon_{i,+} = \varepsilon_{i,-} = \varepsilon_0$, and $t_{i,+} = t_{i,-} = t_0$. In Figures 2(a) and 2(b), we show the thermal conductance spectra κ for several DNA structures with different chain length N. As expected, the thermal conductance displays as a clear antiresonance valley with a zero point at the Fermi level for the structure with $N = 1$. This is ascribed to the Fano antiresonance originating from the destructive interference between the non-localized states in the base pairs along the main conductance channel and the localized states in the upper and lower backbones. Meanwhile two resonance peaks appear at the energies corresponding to the bonding and antibonding "molecular states", i.e., the superradiant states in upper and lower backbones. As N increases, both edges of the valley become steep rapidly, and as N increases to a not very large value, for example $N = 4$, the valley is much

suppressed to a well-defined adiabatic band, where the thermal flux is forbidden to flow through the DNA chain. Moreover, these antiresonance and resonance characteristics also appear in the corresponding electronic conductance spectra G as shown in Figures 2(c) and 2(d). Nevertheless, as N increase, the difference becomes obvious in the resonances near to the both edges of the antiresonance valley. In order to clearly see the influence of the Fano antiresonance on thermoelectric properties of the DNA system, we compare Lozentz ratio $L = \kappa/GT$ with Lorentz number $L_0 = (k_B\pi)^2/3e^2$ in Figures 2(e) and 2(f). It can be found that Lorentz ratio strongly deviates from Lorentz number in the vicinity of the antiresonance point, indicating a strong violation of the WF law. Moreover, such a violation becomes stronger as the DNA chain length increases. In particular, L also deviates from L_0 in the vicinity of superradiant states, i.e., $\varepsilon_0 = \pm t_0$.

The quantum interference has a significant impact on the thermopower S and the figure of merit ZT as well. The thermopower S, shown in Figures 2(g) and 2(h), has one zero point corresponding to Fano antiresonance point in the spectrum of thermal conductance as N is small. As N increases, two additional zero points appear in the vicinity of the superradiant states, as shown in Figure 2(g). Whenever ε_0 passes these three zero points, the thermopower S changes its sign and displays as an antisymmetric behavior due to the electron-hole symmetry.[55,56] When the level ε_0 is above one of these zero points the main carriers are electrons and then the thermopower is negative. When ε_0 is below the zero point the main carriers are holes and thus the thermopower is positive. Obviously, a considerable enhancement of the thermopower appears in the vicinity of the antiresonance points since the transmission function changes sharply near these points. Besides, the figure of merit ZT develops double peaks around the level $\varepsilon_0 = 0$, and their maximum values increase with increasing N as shown in Figures 2(i) and 2(j), indicating that the Fano antiresonance enhances the thermoelectric efficiency of the DNA system remarkably. In addition, we also find that ZT is also enhanced in the vicinity of superradiant states, which ascribes to the weighted symmetry in the location of the bonding and antibonding states with respect to the Fermi level. That is to say, the

current due to electrons tunneling thought the bonding state is compensated by the current due to holes tunneling through the antibonding level.[54] This is just a local bipolar effect in the backbones of the DNA molecules.

Considering the intrinsic double helix confirmation of the DNA molecule, the upper and lower backbones are no longer symmetrical to the GC base pairs due to the environmental complications or fluctuations.[30] To simulate such a characteristic, we assume the energies in the upper and lower backbones are no longer uniform by an energy difference Δ, i.e., $\varepsilon_{i,+} = \varepsilon_0 - \Delta$ and $\varepsilon_{i,-} = \varepsilon_0 + \Delta$. In Figure 3 we show the thermoelectric and electric transports through the DNA molecule with $\Delta = 0.5t_0$ and various chain lengths. It is clear that some additional resonance peaks appear at $\varepsilon_0 = 0$ in both the thermal conductance spectra κ (see Figure 3(a) and 3(b)) and the electronic conductance spectra G (see Figure 3(c) and 3(d)). Meanwhile two Fano antiresonance points with zero value appear at $\varepsilon_0 = \pm\Delta$ in them. These additional central peaks around $\varepsilon_0 = 0$ arise from the subradiant state and are analogous to the Dicke effect in quantum optics,[39,40] thus we refer to it as Dicke resonances. As the DNA chain length increases, the Dicke resonance peak develops to a resonance plateau characterized by very step edges in the thermal conductance spectra κ while by several small sharp peaks in the electronic conductance spectra G. Moreover, the appearance of the Dicke resonance plateau indicates that the energy difference due to the environment complications or fluctuations induces the adiabatic-diabatic transition in the DNA molecule. As for electronic transport through the DNA system, it indicates a semiconducting-metallic transition. This may give a qualitative explanation for the experimental observation the conductance of the DNA molecule increases with the increasing of salt concentration and *p*H, and a larger current is observed at ambient conditions than in vacuum conditions.[57] Similar to the discussions above, Lorentz ratio is also calculated and shown in Figures 3(e) and 3(f). One can see that in the WF law is not only strongly violated at two zero points $\varepsilon_0 = \pm\Delta$, but also violated in the vicinities of the superradiant

state and the subradiant state due to the Dicke effect. Moreover, these violations become stronger as N increases, indicating that the Dicke effect is more pronounced. As expected, the thermopower S, shown in Figures 3(g) and 3(h), has six zero points. Two of them correspond to the Fano antiresonance points $\varepsilon_0 = \pm\Delta$, and the other four zero points correspond to the resonance points in the vicinities of the subradiant states and the superradiant states in the DNA molecule. For non vanishing Δ, the spectrum of ZT is mainly dominated by two double-peak structures in the vicinity of the two antiresonance points on both sides of the Fermi level, as shown in Figures 3(i) and 3(j). In the vicinities of two antiresonace points and four resonance points, ZT is much enhanced, and meanwhile is enhanced further by the increasing of the DNA chain length.

To shed a more detailed light on the Dicke effect in the thermoelectric coefficients of the DNA molecule, we need change the energy difference Δ in the upper and lower backbones. Here we take the DNA molecule with N = 5 as an example. The corresponding numerical results are shown in Figure 4. It is obvious that for a small level shift Δ ~ 0, a sharp Dicke peak appears at $\varepsilon_0 = 0$ in both the thermal conductance spectrum κ (see Figure 4(a)) and the electric conductance spectrum G (see Figure 4(c)), and the DOS exhibits a δ-like shape at the level $\varepsilon_0 = 0$, indicating a semiconducting-metallic transition in electronic transport. Moreover, as Δ increases, the width of the Dicke peak becomes large, as shown in Figures 4(a)-4(d). For a small value of Δ, the subradiant state and the Fano antiresonance points are close to each other, the WF law is much strongly violated (see Figure 4(e)), while as Δ increases to a relatively large value, the subradiant state is far away from the both sides of the Fano antiresonance points. As a result, the thermopower S increases sharply near the subradiant state with increasing Δ (see Figure 4(g)), while decreases as Δ increases further (see Figure 4 (h)). Due to the strong violation of the WF law as the Fano antiresonance points are close to the Dicke resonance ones, a giant enhancement in ZT high to 1.2×10^3 is observed in the DNA molecule for $\Delta \sim 0.1t_0$, as shown in Figure 4(i), while as Δ increases across this value, the maximum value of ZT increases sharply (see Figure 4(j)). It should be noted that to achieve such an

enhancement in *ZT* does not need a large energy difference between the upper backbone and the lower one. Such a relatively small energy difference tends to occur in a realistic DNA molecule by the environmental fluctuations. These results put forward a new route to realize high figure of merit in the DNA molecule.

Intrinsic double helix confirmation of the DNA molecule and the environmental fluctuations may induce another phenomenon, i.e., the symmetry of the electronic hoppings between the backbones and the GC pair bases is broken. To determine the influence of the asymmetric hoppings on the electric and the thermoelectric properties of the DNA molecule, we take the DNA molecule with energy difference parameter $\Delta = 0.5t_0$ as an example, in which the hopping parameters are set as $t_{v,+} = t_0 (1- \eta)$ and $t_{v,-} = t_0 (1+ \eta)$, where η denotes the asymmetry strength of the upper and lower electron hopping. The numerical results are shown in Figure 5, where η is changed from zero to 1. First, one can find that as η increases, the central Dicke resonance plateaus in both the thermal conductance spectra κ and the electronic conductance spectra G becomes narrow progressively, and meanwhile shift towards high-energy direction, as shown in Figures 5(a)-5(d). As η increases to its maximum value, which means that $t_{v,+}$ is turned out from the system while $t_{v,-}$ reaches its maximum value of $2t_0$, one can find that the Dicke resonance peak disappears from the thermal and electronic conductance spectra, which means that two or more dangling side radicals with difference energies coupled with the base pairs is a crucial condition for occurrence of the Dicke resonance in the DNA molecule and similar systems.

Under current circumstances, two Fano antiresonance points are still located at $\varepsilon_0 = \pm\Delta$ symmetrically. However, the L/L_0 spectra are no longer symmetrical about Fermi level, and the violation of the WF law is more stronger at $\varepsilon_0 = \Delta$ than that at $\varepsilon_0 = -\Delta$ as shown in Figures 5(e) and 5(f), because the subradiant state due to the Dicke effect is close to the antiresonance point $\varepsilon_0 = \Delta$. Moreover, just due to the same reason, the thermopower S and the figure of merit ZT are no longer symmetrical about the Fermi level as shown in Figures 5(g)-5(j). It is clearly shown that the shapes

of S and ZT around the antiresonance point $\varepsilon_0 = -\Delta$ show little changing with various η. While around another resonance point $\varepsilon_0 = \Delta$, for a small value of η, the thermopower S and the figure of merit ZT are enhanced to very large values compared to the cases of $\Delta = 0.5t_0$ and $\eta = 0$ shown in Figure 3. Nevertheless, as η increases, the values of S and ZT in the vicinity of $\varepsilon_0 = \Delta$ decreases sharply, and as η increases to its maximum value, i.e., $\eta = 1$, the thermopower S and the figure of merit ZT only keep their symmetrical structures about the antiresonance point $\varepsilon_0 = -\Delta$. This is due to the fact that as $\eta = 1$, the upper backbones are entirely detached from the system and show no any influence on the thermoelectric properties of the system. Thus there is only one Fano antiresonance point appearing at $\varepsilon_0 = -\Delta$ in the corresponding thermal conductance and the thermopower spectra. It should be pointed out the giant enhancement in the thermopower and the figure of merit of the DNA system induced by the asymmetrical electronic hoppings between the backbones and the base pairs dose not need a large disturbance in the electronic hoppings, this is easy to realize in a realistic DNA molecule by the environmental fluctuations. It is believed that we obtain another effective route to enhance the thermoelectric efficiency in the DNA molecule.

It should be noted that in the above discussions, the electric thermal conductance is only taken into account, thus we need to give some comments on the influence of the lattice thermal conductance. Considering that device temperature is so low and assuming that the every repeated unit of the DNA molecule is composed of multiple molecules with different structures, the phonons in the system are difficult to propagate and the electron-phonon couplings are also very weak. Moreover, considering that the Fishbone model with a quantum-dot array is adopted as shown in Figure 1, the lattice thermal conductance is mainly contributed by the base pairs in the main transport channel. Thus the lattice thermal conductance can be described roughly by $\kappa_{ph} = \frac{\pi^2 k_B^2 T}{3h} F_s$,[58] which has been successfully applied to calculate the phonon thermal conductance of the silicon nanowires and matches very well with a recent experiment.[59] The dimensionless

scattering factor F_s arises from phonon scattering with surface impurities or quantum dots.[60] The expression κ_{ph} with F_s=1 is the universal lattice thermal in a nanowire as in a phonon wave guide,[61] while κ_{ph} with F_s=0.1 can suitably describe the lattice thermal conductance of a silicon nanowire with surface states.[62] Since the DNA molecule length in our calculations is much smaller than the phonon mean free paths, the lattice thermal conductance is possible to be reduced by one order of magnitude or even more compared with the electric thermal conductance. Therefore, we adopt F_s=0.5 as a suitable parameter to estimate the lattice thermal conductance of the DNA chain, and assume that F_s is independent of the number of the base pairs. We can find that the maximum value of the figure of merit of the DNA chain obtained above, i.e., ZT_{max}≈1200, will be reduced approximately to 16. If we consider further the influence of the electron-phonon couplings, this value will be reduced to a smaller one. In addition, if we consider inelastic scattering, phase-breaking, field radiation[63] and others in the process of the thermal transport through the DNA molecule, the thermal figure of merit will be reduced more. However, the conclusion that the thermoelectric efficiency in the DNA molecules is enhanced remarkably by the Fano and Dickes effects remains. Our results put forward effective routes to enhance the figure of merit of the DNA molecules and other quasi-one-dimensional materials with similar structure configurations, such as carbon nanotubes, graphene nanoribbons and multiple-coupled quantum-dot systems.

IV. Conclusions

In conclusion, we theoretically investigate the thermoelectric transport through the poly(G)-poly(C) NDA molecule. Our results show that due to the particular structure composed of the repeating backbones and base pairs, the quantum interferences play an important role on the thermoelectric properties of the DNA systems, and the Fano and Dicke effects can be considered as two effective routes to enhance the thermopower and the thermoelectric efficiency of the DNA molecule. Due to the destructive quantum interference originating from the difference backbones, the thermal

conductance spectrum shows a Fano antireasonce zero point at Fermi level, while in the vicinity of the Fano antiresonance point, the WF law is strongly violated, thus the thermopower and the figure of merit are enhanced considerably. Considering the environmental complications or fluctuations, an energy difference between the upper and lower backbones in every repeat unit occurs, which leads to a Dicke resonance appearing at the Fermi level in the thermal conductance spectrum. The appearance of the Dicke effect, on the one side, induces the adiabatic-diabatic transition in the thermal conductance in the DNA molecule. On the other side, the Dicke resonance leads to a strong violation of the WF law, thus in the vicinity of the subradiant state due to the Dicke resonance, the thermopower and the figure of merit are also enhanced considerably. More important, through controlling the Fano and the Dicke effects, for example to make the Dicke resonance points close to the Fano antiresonance ones by adjusting the onsite energies in the backbones or the electronic hoppings between the backbones and the base pairs, a giant enhancement in the figure of merit of the DNA molecule is achieved.

Finally, we give an estimation of the magnitude of the DNA device temperature used in our calculations. The first-principle calculations have reported the electronic hopping t_0 between the GC base pairs ranging from 0.03 to 0.4eV,[14,64] the corresponding device temperature k_BT (=0.01t_0) distributes in the region [3.6 K, 48 K]. The temperatures are lower than room temperature but located in the measured temperatures in the most experiments on the DNA molecule, and consistent with the thermoelectric experimental parameters.[65]

Acknowledgments

This work was supported by the National Natural Science Foundation of China (Nos. 10804034 and 11074081), by the Natural Science Foundation of Hubei Province (No. 2008CDB003), and by the National 973 Project under Grant No. 2006CB921605.

References

1 N. C. Seeman, *Nature* (London), 2003, **421**, 427.

2 A.-M. Guo, S.-J. Xiong, Z. Yang and H.-J. Zhu, *Phys. Rev. E*, 2008, **78**, 061922.

3 D. D. Dley and D. I. Spivey, *Trans. Faraday Soc.*, 1962, **58**, 411.

4 A. Yu. Kasumov, M. Kociak, S. Guron, B. Reulet, V. T. Volkov, D. V. Klinov and H. Bouchiat, *Science*, 2001, **291**, 280.

5 H. W. Fink and C. Schonenberger, *Nature*, 1999, **398**, 407.

6 A. Pakitin, P. Aich, C. Papadopoulos, Y. Kobzar, A. S. Vedeneev, J. S. Lee and J. M. Xu, *Phys. Rev. Lett.*, 2001, **86**, 3670.

7 O. Legrand, D. Cote and U. Bockelmann, *Phys. Rev. E*, 2006, **73**, 031925.

8 M. S. Xu, R. G. Endres, S. Tsukamoto, M. Kitamura, S. Ishida and Y. Arakawa, *Small*, 2005, **1**, 1168.

9 E. Shapir, H. Coher, A. Calzolari, C. Cavazzoni, D. A. Ryndyk, G. Cuniberti, A. Kotlyar, R. Di Felice and D. Porath, *Nat. Mater.*, 2008, **7**, 68.

10 S. Roy, H. Vedala, A. D. Roy, D.-H. Kim, M. Doud, K. Mathee, H.-K. Shin, N. Shimamoto, V. Prasad and W. Choi, *Nano Lett.*, 2008, **8**, 26.

11 E. Braun, Y. Eichen, U. Sivan and G. Ben-Yoseph, *Nature* (London), 1998, **391**, 775.

12 P. J. de Pablo, F. Moreno-Herrero, J. Colchero, J. Gómez Herrero, P. Herrero, A. M. Baró, P. Ordejón, J. M. Soler and E. Artacho, *Phys. Rev. Lett.*, 2000, **85**, 4992 (2000).

13 Y. Zhang, R. H. Austin, J. Kraeft, E. C. Cox and N. P. Ong, *Phys. Rev. Lett.*, 2002, **89**, 198102.

14 G. Cuniberti, L. Craco, D. Porath and C. Dekker, *Phys. Rev. B*, 2002, **65**, 241314(R).

15 Y. Zhu, C.-C. Kaun, and H. Guo, *Phys. Rev. B*, 2004, **69**, 245112.

16 D. Klotsa, R. A. Römer and M. S. Turner, *Biophys. J.*, 2005, **89**, 2187.

17 E. Maciá and S. Roche, *Nanotechnology*, 2006, **17**, 3002.

18 A. A. Voityuk, J. Jortner, M. Bixon and N. Rösch, *J. Chem. Phys.*, 2001, **114**, 5614.

19 R. N. Barnett, C. L. Cleveland, U. Landman, E. Boone, S. Kanvah and G. B. Schuster, *J. Phys. Chem. A*, 2003, **107**, 3525.

20 J. Ladik, A. Bende and F. Bogar, *J. Chem. Phys*., 2007, **127**, 055105.

21 A. A. Voityuk, *J. Chem. Phys.*, 2008, **128**, 115101.

22 J. Qi, N. Edirisinghe, M. Golam Rabbani and M. P. Anantram, *Phys. Rev. B*, 2013, **87**, 085404.

23 E. Maciá, *Phys. Rev. B*, 2007, **75**, 035130.

24 W. Zhang, R. Yang and S. E. Ulloa, *Phys. Rev. E*, 2009, **80**, 051901.

25 W. Zhang, R. Yang, Y. Zhao, S. Duan, P. Zhang and S. E. Ulloa, *Phys. Rev. B*, 2010, **81**, 214202.

26 A.-M. Guo and Q.-F. Sun, *Phys. Rev. Lett.*, 2012, **108**, 218102.

27 A.-M. Guo and Q.-F. Sun, *Phys. Rev. B*, 2012, **86**, 115441.

28 A.-M. Guo and S.-J. Xiong, *Phys. Lett. A*, 2008, **372**,3259.

29 J. Yi, *Phys. Rev. B*, 2003, **68**, 193103.

30 B. Göhler, V. Hamelbeck, T. Z. Markus, M. Kettner, G. F. Hanne, Z. Vager, R. Naaman and H. Zacharias, *Science*, 2011, **331**, 894.

31 R. Gutierrez, E. Diaz, R. Naaman and G. Cuniberti, *Phys. Rev. B*, 2012, **85**, 081404(R).

32 D. Rai and M. Galperin, *J. Phys. Chem. C*, 2013, **117**, 13730.

33 R. Naaman and D. H. Waldeck, *J. Phys. Chem. Lett.*, 2012, **3**, 2178.

34 H. H. Fu and K. L. Yao, *Appl. Phys. Lett.*, 2012, **100**, 013502.

35 H. H. Fu and K. L. Yao, *J. Chem. Phys.*, 2011, **134**, 054903.

36 H. H. Fu and K. L. Yao, *J. Appl. Phys.*, 2011, **110**, 094502.

37 B. Kubala, J. König, and J. Pekola, *Phys. Rev. Lett.*, 2008, **100**, 066801.

38 M. Sato, H. Aikawa, K. Kobayshi, S. Katsumoto, Y. Iye, *Phys. Rev. Lett.*, 2005, **95**, 066801.

39 R. H. Dicke, *Phys. Rev.*, 1953, **89**, 472.

40 R. H. Dicke, *Phys. Rev.*, 1954, **93**, 99.

41 Y. J. Yan and H. Y. Zhang, *J. Theor. Comput. Chem.*, 2002, **1**, 225.

42 E. Maciá, *Phys. Rev. B*, 2007, **76**, 245123.

43 H. Y. Zhang, X. Q. Li, P. Han, X. Y. Yu and Y. J. Yan, *J. Chem. Phys.*, 2002, **117**, 4578.

44 A. A. Fouladi and S. A. Ketabi, *J. Supercond. Nov. Magn.*, 2013, **26**, 469.

45 D. Porath, A. Bezryadin, S. de Vries and C. Dekker, *Nature* (London), 2000, **403**, 635.

46 B. Q. Xu, P. M. Zhang, X. L. Li and N. J. Tao, *Nano Lett.*, 2004, **4**, 1105.

47 S. Roche, *Phys. Rev. Lett.*, 2003, **91**, 108101.

48 A. P. Jauho, N. S. Wingreen and Y. Meir, *Phys. Rev. B*, 1994, **50**, 5528.

49 Y. Meir, N. S. Wingreen and P. A. Lee, *Phys. Rev. Lett.*, 1991, **66**, 3048.

50 P. Trocha and J. Barnaś, *Phys. Rev. B*, 2007, **76,** 165432.

51 H. H. Fu and K. L. Yao, *Europhys. Lett.*, 2013, **103,** 57011.

52 Y. Ouyang and J. A. Guo, *Appl. Phys. Lett.*, 2009, **94,** 263107.

53 V. Apraecida da Costa and E. de Andrada e Silva, *Phys. Rev. B*, 2010, **82,** 153302.

54 P. Trocha and J. Barnaś, *Phys. Rev. B*, 2012, **85,** 085408.

55 Q. Wang, H. Xie, Y. -H. Nie and W. Ren, *Phys. Rev. B*, 2013, **87,** 075102.

56 J. Liu, Q.-F. Sun and X. C. Xie, *Phys. Rev. B*, 2010, **81** 245323.

57 H. Vedala, S. Roy, M. Doud, K. Mathee, S. Hwang, M. Jeon and W. Choi, *Nanotechnology*, 2008, **19**, 65704.

58 David M.-T. Kuo and Y. C. Chang, *Phys. Rev. B*, 2010, **81**, 205321.

59 A. I. Hochbaum, R. Chen, R. D. Delgado, W. Liang, E. C. Garnett, M. Najarian, A. Majumdar and P. Yang, *Nature*, 2008, **451**, 163.

60 A. J. Minnich, M. S. Dresselhaus, Z. F. Ren and G. Chen, *Energy Environ. Sci.*, 2009, **2**, 466.

61 K. Schwab, E. A. Henriksen, J. M. Worlock and M. L. Roukes, *Nature*, 2000, **404**, 974.

62 T. Markussen, A. P. Jauho and M. Brandbyge, *Phys. Rev. Lett.*, 2009, 103, 055502

63 L. Hu, A. Narayanaswamy, X. Chen and G. Chen, *Appl. Phys. Lett.*, 2008, **92**, 133106.

64 J. D. Wastson and F. H. Crick, *Nature*, 1953, **171**, 737.

65 R. Scheibner, M. Konig, D. Reuter, A. D. Wieck, H. Buhmann and L. W. Molenkamp, *New J. Phys.*, 2008, **10**, 083016.

Figures and Captions

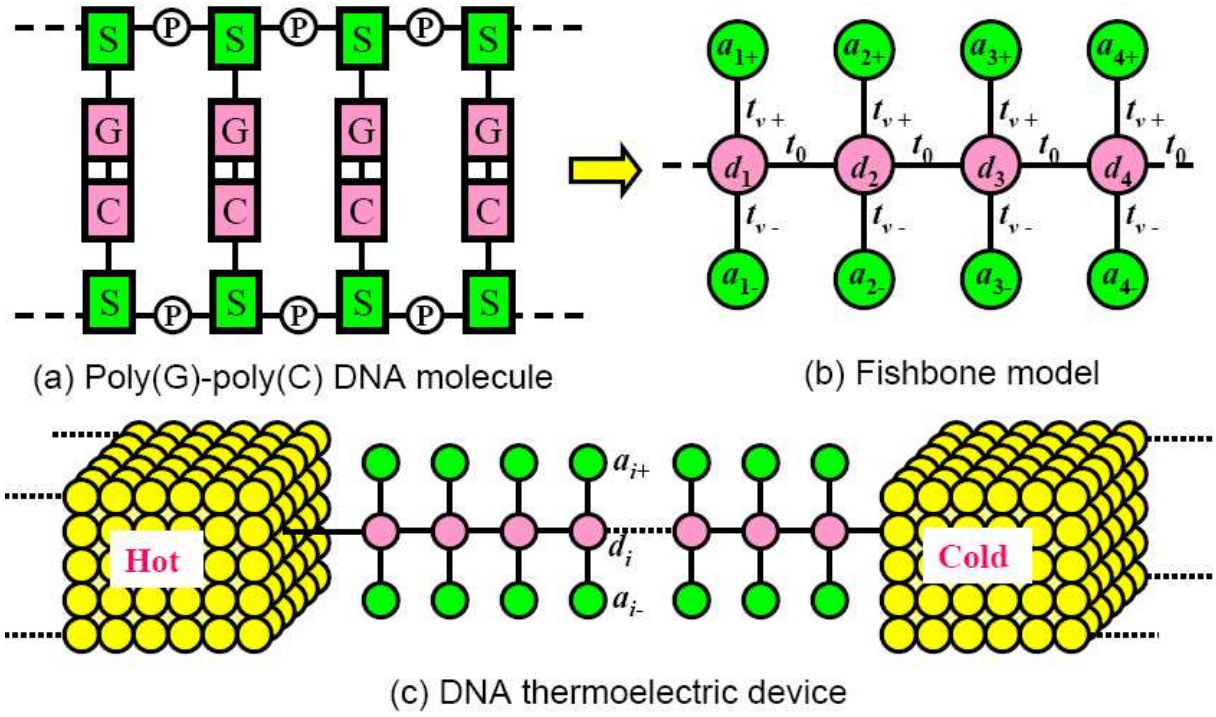

Fig. 1 (a) A schematic view of poly(G)-poly(C) DNA molecule; each GC base pair is attached to sugar and phosphate groups forming the upper and lower molecule backbone. (b) The diagram of the lattice adopted in building a fishbone model, with the π-stack connected to the isolated states as ± edges. (c) A schematic view of a thermoelectric device based on the poly(G)-poly(C) DNA molecule.

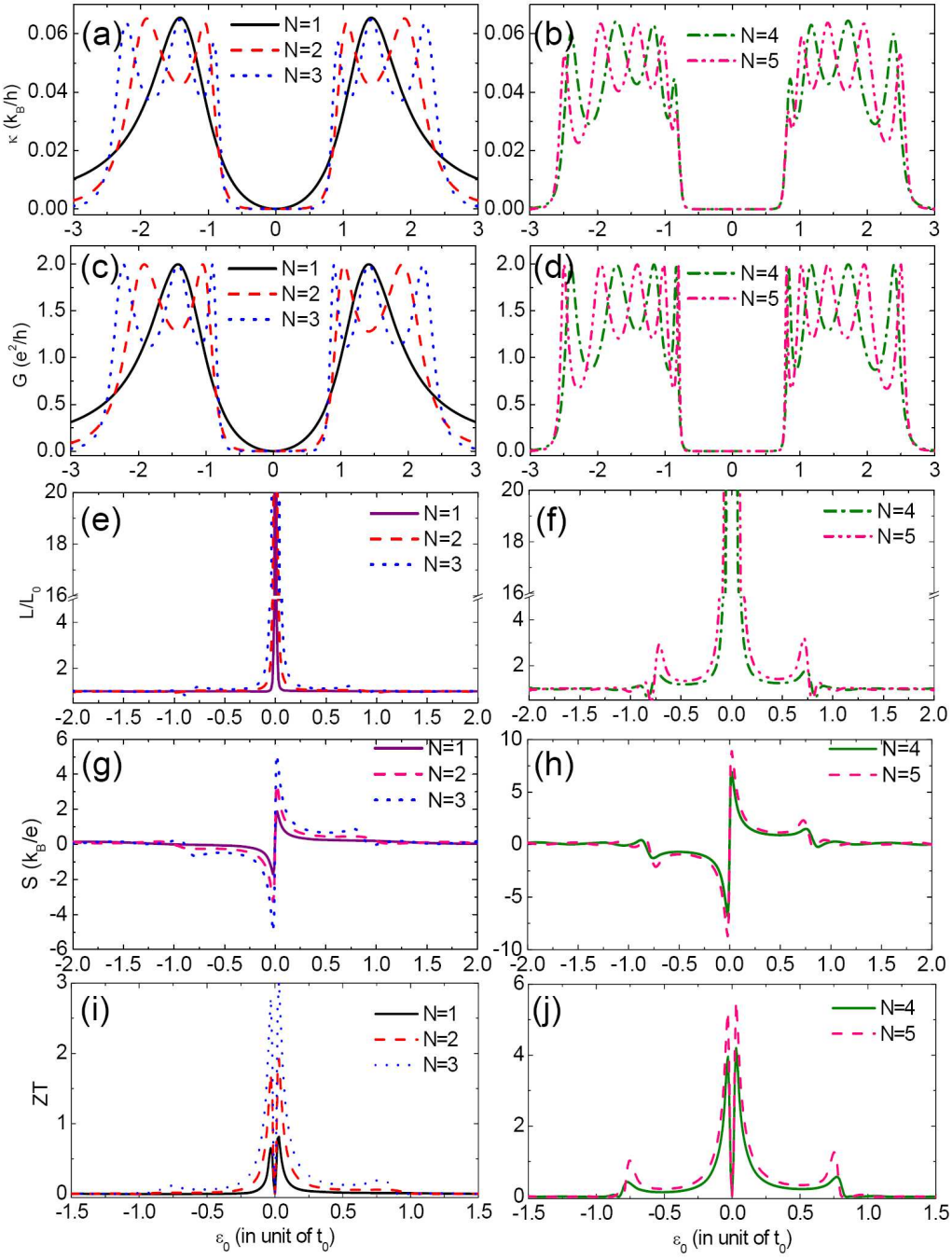

Fig. 2 Thermal conductance κ, Electric conductance G, Lorentz ratio L/L_0, thermopower S and figure of merit ZT as a function of the energy level ε_0 for some DNA molecules with the chain length $N = 1 - 5$, in which the onsite energies in the backbones are set as $\varepsilon_{i,+} = \varepsilon_{i,-} = \varepsilon_h = \varepsilon_0$.

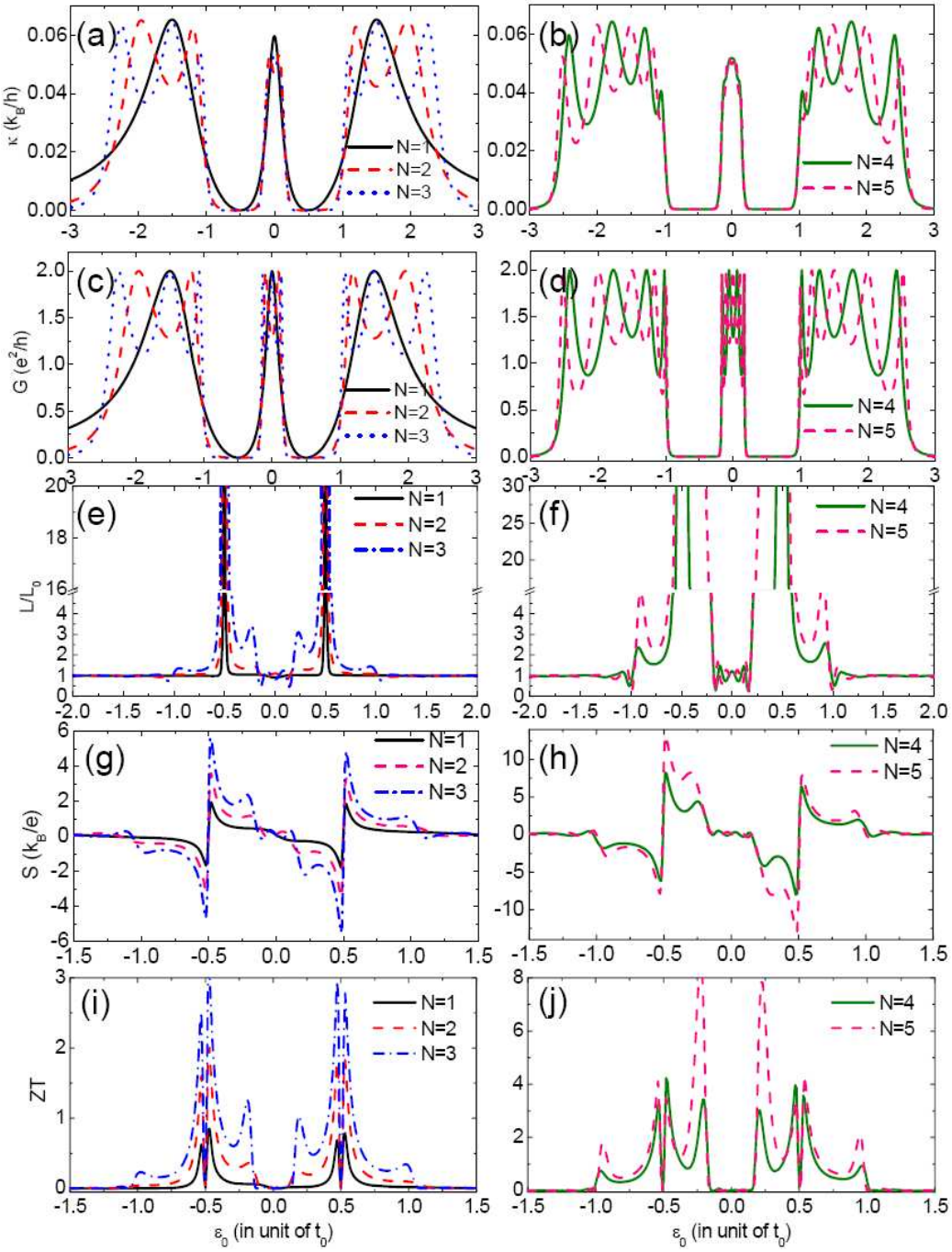

Fig. 3 (Color online) Thermal conductance κ, Electric conductance G, Lorentz ratio L/L_0, thermopower S and figure of merit ZT versus ε_0 for some DNA molecules with the chain length N = 1 – 5, in which the onsite energies backbones are set as $\varepsilon_{i,h} = \varepsilon_0$, $\varepsilon_{i,+} = \varepsilon_0 - \Delta$ and $\varepsilon_{i,-} = \varepsilon_0 + \Delta$, where $\Delta = 0.5t_0$.

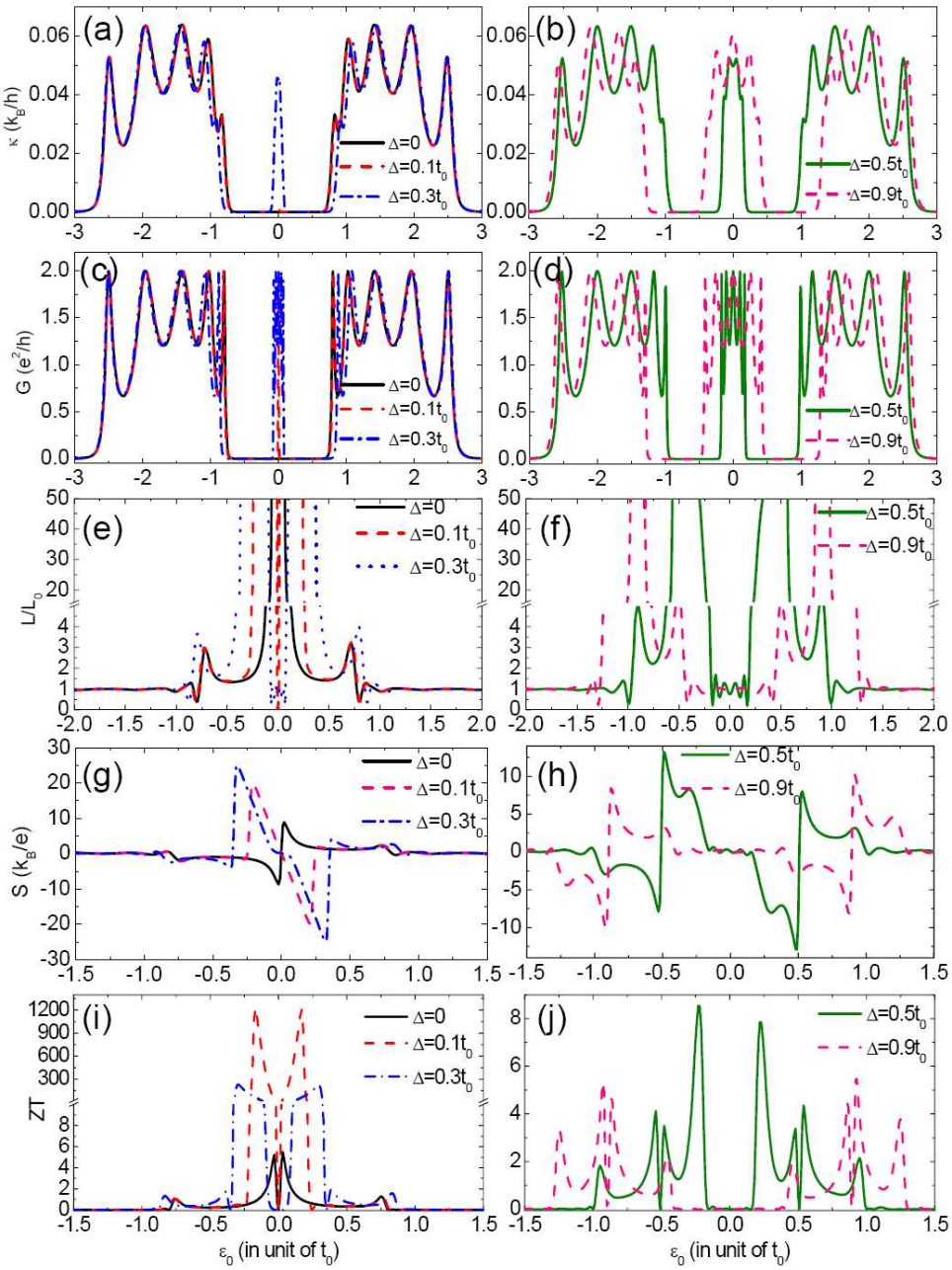

Fig. 4 (Color online) Thermal conductance κ, Electric conductance G, Lorentz ratio L/L_0, thermopower S and figure of merit ZT versus ε_0 for a particular DNA molecule with the chain length $N = 5$, where the onsite energies backbones are $\varepsilon_{i,h} = \varepsilon_0$, $\varepsilon_{i,+} = \varepsilon_0 - \Delta$ and $\varepsilon_{i,-} = \varepsilon_0 + \Delta$, and Δ is changed from 0 to $0.9t_0$.

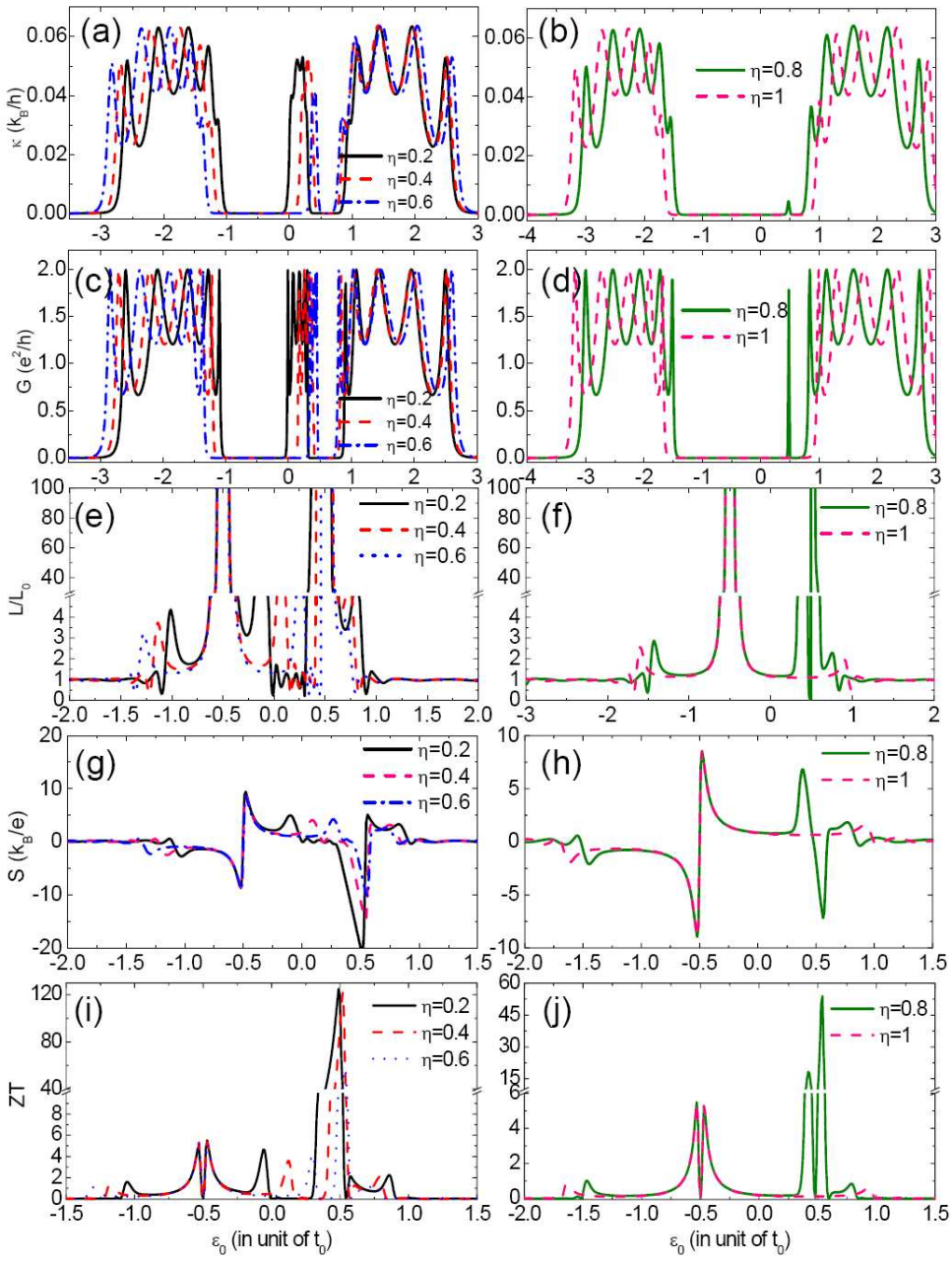

Fig. 5 (Color online) Thermal conductance κ, Electric conductance G, Lorentz ratio L/L_0, thermopower S and figure of merit ZT versus ε_0 for a particular DNA molecule with $N = 5$ and $\Delta = 0.5t_0$, in which the electronic hopping between the backbones and the base pairs is set as $t_{i,+} = t_0 (1- \eta)$ and $t_{i,-} = t_0 (1+ \eta)$, where η is changing from 0 to 1.